Available online at www.sciencedirect.com
SCIENCE DIRECT®
Journal of Sound and Vibration 273 (2004) 1101–1108
JOURNAL OF SOUND AND VIBRATION
www.elsevier.com/locate/jsvi

Letter to the Editor

Non-linear dynamics of an elastic beam under moving loads

A.N. Yanmeni Wayou, R. Tchoukuegno, P. Woafo*

Laboratoire de Mécanique, Faculté des Sciences, Université de Yaoundé I, B.P. 812, Yaoundé, Cameroon

Received 11 March 2003; accepted 1 September 2003

1. Introduction

During the 20th century, many studies were carried out to analyze the dynamics of structures under moving loads. The interest was at the beginning oriented toward bridges and railways to study the conditions under which these structures are stable [1,2]. The principal results show that, compared to a beam under a static load, the load inertia modifies the beam dynamics in two ways: the inertia renders the beam deflection higher, and resonance is reached at a lower moving load velocity [3,4]. Dugush and Eisenberger [5] applied modal analysis in combination with integral transformation methods to determine the dynamic deflection and the internal forces of a multi-span non-uniform beam under moving loads. They showed that a small number of mode shapes are required to obtain accurate solutions. Zhu and Law [6] studied the dynamic loading on a multi-lane continuous bridge due to vehicles moving on top of the bridge deck and highlighted the influence of the transverse vehicle position and road surface roughness on the dynamic impact factor, defined as the ratio of the maximum dynamic response to the maximum static response. Gbadeyan and Oni [7] developed a general approach to determining solutions of both moving force and moving mass problems for both Euler–Bernoulli and Rayleigh beams having any of the classical end-support conditions.

From experiments, it appears that as the amplitude of oscillations increases, non-linear effects come into play; therefore acknowledging that the source of non-linearity may be inertial, geometric or material in nature, the influence of the non-linearity on the beam dynamics should also be highlighted (see Ref. [8] and references therein). In this paper, attention is put on non-linearity which may be caused by large curvatures or non-linear stretching of the mid-plane of a beam. In general, exact solutions for the beam response are not available, so recourse has been to approximate analyses by using purely numerical techniques, purely analytic techniques and numerical–analytic techniques. In the numerical–analytic technique adopted, the displacement is expressed in the form of a combination of the linear free-oscillation modes of the beam. Then, the equations of motion of the modal co-ordinates are obtained and solved by a perturbation technique. Nayfeh and Mook [8] developed an approach to determine the non-linear equation of

*Corresponding author.
E-mail address: pwoafo@uycdc.uninet.cm (P. Woafo).

0022-460X/$ - see front matter
doi:10.1016/j.jsv.2003.09.040

motion of a beam with non-moving loads and obtained a Duffing-like system. In this paper, the moving load inertia is included in the Duffing equation in order to study the non-linear dynamics of a Euler–Bernoulli beam under moving loads so as to handle the influence of both the load inertia and the non-linearity. The method of multiple scales is adopted to highlight the parametric resonance. The influence of the mass parameter, the damping and the load velocity on the beam deflections are examined. Section 2 presents the model, the modal equation and the numerical results. Conclusions are given in Section 3.

2. Model and modes equations

2.1. The model

Consider a beam of length l under a moving load as shown in Fig. 1. In discussing beams, attention is restricted to planar and non-rotating motions. The equations of motion are obtained by a combination of the inertial effect of the moving load [4] and the non-linear effect in the beam dynamics [8]. Assuming that plane sections remain plane and a linear stress–strain law, the equations of motion governing the non-linear dynamics of a beam with uniform shape subjected to a moving load of mass M and velocity v are given by

$$\rho S u_{tt} - ES u_{xx} = \tfrac{1}{2}(ES)\frac{\partial}{\partial x}[(1-2u_x)y_x^2], \tag{1}$$

$$\rho S y_{tt} + EI y_{xxxx} + c y_t + M\delta(x-vt)\{y_{tt} + 2v y_{xt} + v^2 y_{xx}\} = F(t)\delta(x-vt) + ES\frac{\partial}{\partial x}(e y_x), \tag{2}$$

where

$$e = u_x - u_x^2 + \tfrac{1}{2}y_x^2. \tag{3}$$

In these equations E is Young's modulus of the beam, ρ is the beam density, S, I are, respectively, the area and moment of inertia of the beam cross-section. $y(x,t)$ is the vertical deflection of the beam, while u is the axial displacement, y and u depend on the spatial co-ordinate x and the time t. The subscripts nt and nx stand for the nth order derivative with respect to t and x. $F(t) = Mg$ is the force due to the moving load where g is the acceleration due to the gravity. c is the damping which is assumed to be constant. $\delta(\cdot)$ is Dirac's delta function and illustrates the fact that the position of the load changes with time. The inertial effect of the moving load is shown in Eq. (2) by the presence of the fifth term. In the absence of this term, the system is familiar as a beam under a moving force. The last term in Eq. (2) indicates that the motion is non-linear.

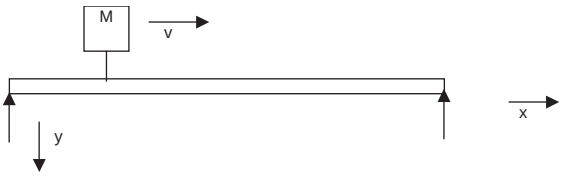

Fig. 1. Beam under moving load.

At this point, it is convenient to introduce dimensionless variables:

$$X = \frac{x}{l}, \quad \tau = vt/l, \quad Y = \frac{y}{l}, \quad U = \frac{u}{l}.$$

Consider a hinged–hinged beam and assume that the longitudinal inertial terms u_{tt} and u_x^2 are negligible (case of beam with small radius of gyration). Eqs. (1) and (2) reduce to

$$Y_{\tau\tau} + \frac{EI}{mv^2} Y_{xxxx} + 2\mu' Y_\tau + \frac{M}{m} \delta[l(x-\tau)](Y_{\tau\tau} + 2Y_{x\tau} + Y_{xx}) = \left(\frac{E}{2\rho v^2} \int_0^1 Y_x^2 \, \mathrm{d}x\right) Y_{xx} + F(x,\tau), \tag{4}$$

where

$$2\mu' = cl/mv, \quad F(x,\tau) = M\, lg\, \delta[l(x-\tau)]/mv^2 \quad \text{and} \quad m = \rho S. \tag{5}$$

2.2. Mode equations

It is convenient to assume an expansion for the deflection Y in terms of the combination of the linear free-oscillation modes, which are those of a hinged–hinged beam in this case. Thus, an expansion is assumed for Y in the form

$$Y(X,\tau) = \sum_{n=1}^{\infty} Y_n(\tau)\phi_n(X), \tag{6}$$

where $\phi_n(X) = \sin(n\pi X)$ is the natural mode of a hinged–hinged beam.

Substituting Eq. (6) into Eq. (4), multiplying by $\sin(j\pi X)$ and integrating over the interval [0,1] leads to the mode equations

$$\ddot{Y}_j + \omega_j^2 Y_j = -\epsilon \left[2 \sum_{n=1}^{\infty} (\ddot{Y}_n \sin n\pi\tau + 2\dot{Y}_n n\pi \cos n\pi\tau - n^2\pi^2 Y_n \sin n\pi\tau) + 2\eta\omega_j \dot{Y}_j + \frac{j^2\pi^4 b}{4} Y_j \sum_{n=1}^{\infty} n^2 Y_n^2 - 2K \sin(j\pi\tau) \right]. \tag{7}$$

$\epsilon = M/ml$ is the non-dimensional parameter describing the ratio of the moving load mass M to the mass of the beam given by

$$\rho \cdot S \cdot l \cdot \omega_j = \frac{(j\pi)^2}{vl} \sqrt{\frac{EI}{m}}, \quad \epsilon b = \frac{E}{\rho v^2}, \quad K = \frac{gl}{v^2}, \quad 2\mu' = 2\bar{\eta}\omega_j = 2\eta\epsilon\omega_j.$$

A solution of Eq. (7) is sought by the method of multiple scales. Accordingly, the solution is expressed in terms of different time scales as

$$Y_j(\tau,\epsilon) = Y_{j0}(\tau_0,\tau_1) + \epsilon Y_{j1}(\tau_0,\tau_1), \tag{8}$$

where $\tau_m = \epsilon^m\tau$, i.e., $\tau_0 = \tau$ and $\tau_1 = \epsilon\tau$ represents different independent time scales. Substituting in Eq. (7), and noting that $\mathrm{d}/\mathrm{d}\tau = D_0 + \epsilon D_1 + \cdots +, \mathrm{d}^2/\mathrm{d}\tau^2 = D_0^2 + 2\epsilon D_0 D_1 + \cdots$, where $D_0 =$

$\mathrm{d}/\mathrm{d}\tau$, $D_1 = \mathrm{d}/\mathrm{d}\tau_1$, the following set of linear ordinary differential equations result:

$$\epsilon^0: D_0^2 Y_{j0} + \omega_j^2 Y_{j0} = 0, \tag{9}$$

$$\begin{aligned}\epsilon^1: D_0^2 Y_{j1} + \omega_j^2 Y_{j1} = & -2\mathrm{i}\,\omega_j(D_1 A_j \exp(\mathrm{i}\,\omega_j\tau_0) + \mathrm{c.c}) - 2\eta\omega_j^2(\mathrm{i}A_j \exp \mathrm{i}\omega_j\tau_0 + \mathrm{c.c}) \\ & -\frac{1}{2}\left[\sum_{n=1}^{\infty}(\omega_n^2 + n^2\pi^2)(A_n \exp(\mathrm{i}\,\omega_n\tau_0) + \mathrm{c.c})\{\exp(\mathrm{i}(n+j)\pi\tau_0) - \exp(\mathrm{i}(n-j)\pi\tau_0) + \mathrm{c.c}\}\right. \\ & \left. + 2n\pi\ \omega_n(\mathrm{i}A_n \exp(\mathrm{i}\,\omega_n\tau_0) + \mathrm{c.c})\{\mathrm{i}\exp(\mathrm{i}(n-j)\pi\tau_0) - \mathrm{i}\exp(\mathrm{i}(n+j)\pi\tau_0) + \mathrm{c.c}\}\right] \\ & -(\mathrm{i}K \exp(\mathrm{i}j\pi\tau_0) + \mathrm{c.c}) - \frac{b}{4}\pi^4 j^2\left(A_j\left[\sum_{n=1}^{\infty} n^2[An^2 \exp \mathrm{i}(\omega_j + 2\omega_n)\tau_0\right.\right. \\ & \left.\left. + \bar{A}_n^2 \exp \mathrm{i}(\omega_j - 2\omega_n)\tau_0 + 2A_n\bar{A}_n \exp(\mathrm{i}\omega_j\tau_0)\right] + \mathrm{c.c}\right).\end{aligned} \tag{10}$$

Eq. (10) is obtained by substituting the solution of Eq. (9) taken as $Y_{j0} = A_j \exp(\mathrm{i}\omega\tau_0) + \mathrm{c.c.}$ where A_j is a complex amplitude yet to be determined, c.c. stands for the complex conjugate and $\mathrm{i} = (-1)^{1/2}$.

Inspection of Eq. (10) shows that only a parametric resonance with $\omega_j \approx j\pi$ is possible. The internal resonance cannot be possible here because the equations $\omega_j \approx j\pi$ and $\omega_n \approx n\pi$ cannot be satisfied for $n \neq j$, for a single value of the moving load velocity. At the resonance, the corresponding velocity is given by

$$v = \frac{(j\pi)^2}{\omega_j l}\sqrt{\frac{EI}{\rho S}} = \frac{j\pi}{l}\sqrt{\frac{EI}{\rho S}},$$

so $\omega_j \approx j\pi$ and $\omega_n \approx n\pi$ could not be possible for the same velocity if $n \neq j$.

From Eq. (10) it can be seen that as ω_j approaches $j\pi$, secular terms develop. As one is looking for bounded solutions, these terms are to be eliminated.

Putting

$$j\pi = \omega_j + \epsilon\delta_j, \tag{11}$$

δ_j is a parameter to quantify the divergence between $j\pi$ and ω_j. Equating the secular terms to zero leads to the condition on A_j given by

$$\begin{aligned}2\mathrm{i}\,\omega_j D_1 A_j = & -2\mathrm{i}\eta\omega_j^2 A_j - \tfrac{1}{2}\{(\omega_j - j\pi)^2\bar{A}_j \exp(2\,\mathrm{i}\,\varepsilon\delta_{j\tau_0}) - 2(\omega_j^2 + (j\pi)^2)A_j\} \\ & -\tfrac{3}{4}b\pi^4 j^2 A_j^2\bar{A}_j - \mathrm{i}K \exp(\mathrm{i}\,\varepsilon\delta_j\tau_0).\end{aligned} \tag{12}$$

Noting that A_j is independent of τ_0 and assuming A_j to be of the form

$$A_j = \tfrac{1}{2}a_j \exp(\mathrm{i}\theta_j). \tag{13}$$

Eq. (12) results in two first order differential equation for each amplitude and transformed phase $\varphi_j = \epsilon\delta_j\tau_0 - \theta_j$ with $j = 1, 2, 3\ldots$.

$$\omega_j\dot{a}_j = -\epsilon\eta\omega_j^2 a_j - 0.25\epsilon(\omega_j - j\pi)^2 a_j \sin 2\varphi_j - \epsilon K \cos\varphi_j, \tag{14}$$

$$\omega_j a_j \dot{\varphi}_j = \epsilon\omega_j\delta_j a_j - 0.25\epsilon(\omega_j - j\pi)^2 a_j \cos 2\varphi_j + 0.5\epsilon(\omega_j + j^2\pi^2)a_j - \epsilon\tfrac{3}{32} b\pi^4 j^2 a_j^3 + \epsilon K \sin\varphi_j. \quad (15)$$

Eqs. (14) and (15) can be integrated to obtain a_j and φ_j for each modal response. The solution of each mode is given by

$$Y_j(\tau,\varepsilon) = a_j \cos(j\pi\tau - \varphi_j) + \epsilon\left[\frac{(\omega_j + j\pi)a_j}{8j\pi}\cos(3j\pi\tau - \varphi_j) + \frac{b\pi^4 j^4 a_j^3}{128\omega_j^2}\cos(3j\pi\tau - 3\varphi_j)\right]. \quad (16)$$

It is obvious that the transient response of each mode in the case of the linear dynamics of an elastic beam under moving loads can also be obtained easily from theses equations by putting $b = 0$.

2.3. Numerical results

For the numerical simulation, the following data are used: $E = 200 \times 10^9$ N/m^2, $\rho = 7850$ kg/m^3 (steel), $l = 10$ m; $\eta = 0.033$; $S = 0.01$ m^2 or 0.0055 m^2. It is assumed that the cross-section of the beam is a square.

Eqs. (14) and (15) are numerically solved to determine the values a_j and φ_j which are replaced in Eq. (16) to obtain the modal co-ordinate.

Figs. 2 and 3 show the beam deflection for the three first modes; each curve is obtained at the corresponding resonance velocity (first mode: $v = 46.64$ m/s, second mode: $v = 93.28$ m/s, third mode: $v = 139.92$ m/s). In Fig. 3, one can observe that the deflection of the second mode is equal to zero accordingly with Eq. (6) where $\phi_n(X)$ is equal to zero for $n = 2$ and $X = 0.5$. It is obvious that the first mode leads to the highest deflection compared to the second and the third modes. Because one is interested in the influence of the non-linearity and the inertia of the moving load on the beam deflection, only the first mode will be considered in the analysis which follows.

Fig. 4 shows the inertial effect of the moving load. In this figure, the response of the beam is compared with that of a beam under a moving force. It is observed that the maximum amplitude

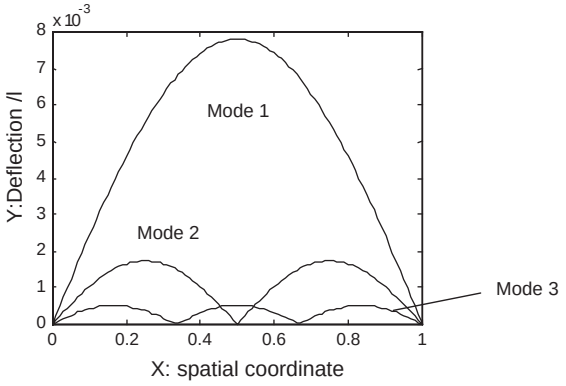

Fig. 2. Beam deflection, variation with X; $\eta\epsilon = 0.01$, $\epsilon = 0.3$, $\tau = 1$; $\delta_j = -2.5$ (resonance velocities—first mode: $v = 46.64$ m/s, second mode: $v = 93.28$ m/s, third mode: $v = 139.92$ m/s).

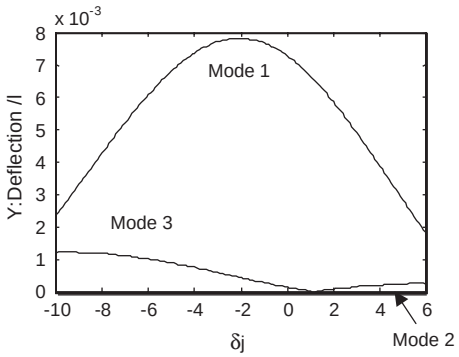

Fig. 3. Beam deflection, variation with δ_j; $X = 0.5$, $\eta\epsilon = 0.01$, $\epsilon = 0.3$, $\tau = 1$, (resonance velocities—first mode: $v = 46.64$ m/s, second mode: $v = 93.28$ m/s, third mode: $v = 139.92$ m/s). The deflection of the beam in the second mode is equal to zero according to Eq. (6) where $\phi_n(X) = 0$ for $n = 2$ and $X = 0.5$.

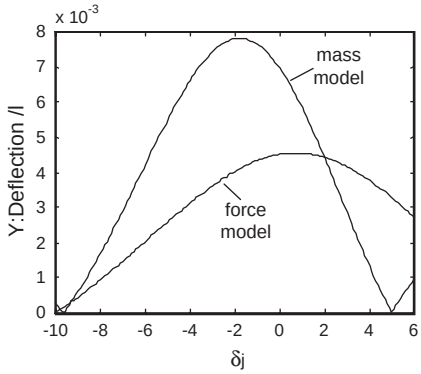

Fig. 4. Beam deflection, variation with δ_j: force and mass models,.$X = 0.5$, $\eta\epsilon = 0.01$, $\epsilon = 0.3$, $\tau = 1$.

of the beam is most significant when the load inertia is taken into account. Note also that the parameter δ_j leading to the highest value of the deflection is low compared to the moving force model. In other words, the resonance occurs at lower moving load velocities for the moving mass model. The mass parameter ϵ and the damping coefficient η also influence significantly the deflection of the beam. As shown in Fig. 5, as ϵ increases, the deflection of the beam grows bigger. But when η grows, the deflection of the beam decreases (this is obvious because in practical situations, the deflection of beams can be reduced by acting on the damping).

Fig. 6 shows the beam deflection for various materials (steel: $E = 200 \times 10^9$ N/m^2, $\rho = 7850$ kg/m^3, iron: $E = 196 \times 10^9$ N/m^2, $\rho = 7800$ kg/m^3, cement/concrete: $E = 45 \times 10^9$ N/m^2, $\rho = 2400$ kg/m^3, wood: $E = 16 \times 10^9$ N/m^2, $\rho = 800$ kg/m^3). It can be observed that steel and iron give way to low deflection compared to that of wood. This is one of the reasons why they are the most used in mechanical or civil engineering. In Fig. 7, the response of the beam in the case of non-linear dynamics is compared with that of linear dynamics (by setting $b = 0$ in this limit); in this case the cross-section S is equal to 0.0055 m^2 (note that the coefficient b depends on S

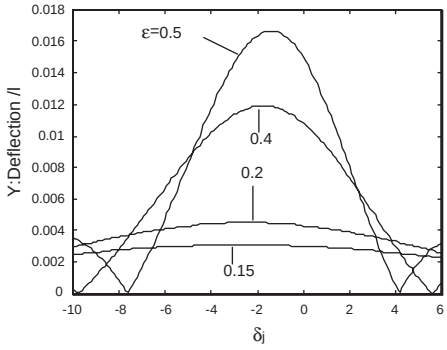

Fig. 5. Beam deflection, variation with δ_j: inertial effect,.$X = 0.5$, $\eta = 0.033$, $\tau = 1$.

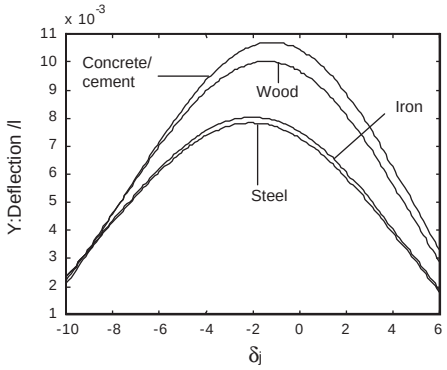

Fig. 6. Beam deflection, variation with δ_j: deflection for various materials,.$X = 0.5$, $\eta\epsilon = 0.01$, $\epsilon = 0.3$, $\tau = 1$.

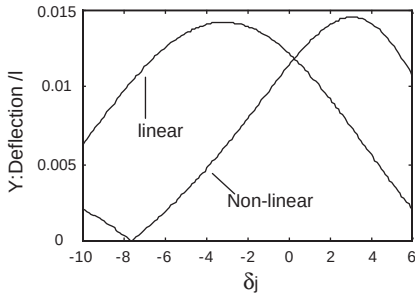

Fig. 7. Beam deflection, variation with δ_j (linear and non-linear cases); $X = 0.5$, $\eta\epsilon = 0.01$, $\epsilon = 0.3$, $\tau = 1$, $S = 0.0055\ \mathrm{m}^2$.

accordingly with the relation $\epsilon b = E/\rho v^2$ where $\epsilon = M/\rho SI$). It is obvious from Fig. 7 that the non-linearity contributes to a relative increase of the maximum deflection and the velocity at the resonance.

3. Conclusions

The analysis carried out and the results obtained in this paper lead to the following conclusions:

The load inertia is to be taken into account in the study of structures under moving load. It can only be neglected under two conditions:

- When the load velocity is higher than that which leads to the resonance in the beam.
- When the moving mass is very small compared to the mass of the beam.

When non-linearity comes into play, the beam deflection and the resonance velocity of the moving load increase.

To avoid high deflection of the beam, the load velocity should be high enough to prevent resonance of the first mode.

References

[1] E.C. Ting, M. Yener, Vehicle structure interactions in bridge dynamics, *Shock Vibration Digest* 15 (1983) 3–9.
[2] D.G. Duffy, The response of an infinite railroad track to a moving vibrating mass, *Transactions of the American Society of Mechanical Engineers, Journal of Applied Mechanics* 57 (1990) 66–73.
[3] J.E. Akin, M. Mofid, Numerical solution for response of beams with moving mass, *Journal of Structural Engineering* 115 (1989) 120–131.
[4] R.G. Rao, Linear dynamics of an elastic beam under moving loads, *Journal of Vibration and Acoustics* 122 (2000) 281–289.
[5] Y.A. Dugush, M. Eisenberger, Vibration of non-uniform continuous beams under moving loads, *Journal of Sound and Vibration* 254 (2002) 911–926.
[6] X.Q. Zhu, S.S. Law, Dynamic load on continuous multi-lane bridge deck from moving vehicles, *Journal of Sound and Vibration* 251 (2002) 697–716.
[7] J.A. Gbadeyan, S.T. Oni, Dynamic behaviour of beams and rectangular plates under moving loads, *Journal of Sound and Vibration* 182 (1995) 677–695.
[8] A.H. Nayfeh, D.T. Mook, *Non Linear Oscillations*, Wiley-Interscience, New York, 1979.